09

Limitation of laser radiation power by carbon materials with a nonlinear optical threshold effect at a flat-top pulse shape

© M.S. Savelyev,[1,2] P.N. Vasilevsky,[1] Yu.P. Shaman,[3] A.Yu. Tolbin,[4] A.Yu. Gerasimenko,[1,5] S.V. Selishchev[1]

[1] Institute of Biomedical Systems, National Research University of Electronic Technology, MIET,
Moscow, Zelenograd, Russian Federation
[2] Institute for Regenerative Medicine, Sechenov First Moscow State Medical University, Sechenov University,
Moscow, Russian Federation
[3] Scientific-Manufacturing Complex „Technological Centre“,
Moscow, Zelenograd, Russia
[4] Institute of Physiologically Active Compounds at Federal Research Center of Problems of Chemical Physics and Medicinal Chemistry, Russian Academy of Sciences,
Chernogolovka, Moscow region, Russia
[5] Institute for Bionic Technologies and Engineering, Sechenov First Moscow State Medical University, Sechenov University,
Moscow, Russia
e-mail: savelyev@bms.zone

Received December 23, 2022
Revised December 23, 2022
Accepted December 23, 2022

The possibilities of using multivariate determination of carbon nanotubes properties based on the dependence data of the normalized transmission logarithm on the sample displacement in the case of Z-scan with an open aperture as well as on the total pulse energy in the case of fixed sample position measurements are studied. The radiation transfer equation for the threshold dependence of the absorption coefficient on the intensity of a flat-top laser beam is used. The data of physical and computational experiments showed the sensitivity of the measured curves with respect to the values of the constants of the optical and threshold energy fluence, as well as the beam waist radius. The possibility of multivariate determination of the properties of liquid carbon nanotube-based dispersed media with a nonlinear optical threshold effect and beam waist radius inside such samples has been established.

Keywords: optical limiting, multivariate analysis, carbon nanotubes, *Z*-scan

DOI: 10.21883/TP.2023.04.55939.281-22

Introduction

The development of perfect passive limiters of laser radiation power based on nonlinear optical threshold phenomena requires creating novel materials whose properties are to be determined using models that consider the laser radiation profile. In this paper, we study disperse media of carbon nanotubes using a new model based on the radiative transfer equation for the threshold dependence of the absorption coefficient on the radiation intensity in the case of a flattop pulsed beam. Earlier, nonthreshold [1,2] and threshold [3] models have been mainly considered only for the case of a pulsed beam with Gaussian shape. For the general case, no analytical solution could be obtained. Such a solution exists only in the particular case of small nonlinear absorption coefficient and small nonlinear attenuation of laser radiation in the nonthreshold model [1]. In the general case, the problem can be solved only numerically [3,4], which requires high-performance computing.

Flattop beams possess constant intensity over the cross section [5,6], which, in turn, leads to a transmission change in the process of nonlinear interaction as compared to Gaussian beams. In the present paper, an exact solution in terms of elementary function is obtained for the first time for a flattop beam in the threshold model, which substantially simplifies all calculations. As a result, we determined the coefficient of nonlinear effective absorption (β_{eff}) and the threshold intensity I_{thr}, as well as the range, in which the variation of laser radiation power obeys the Bouguer–Lambert law and the absorber has the transmission coefficient not less than 70%. The threshold model is a particular case of the nonthreshold one and reduces to it when $I_{\text{thr}} = 0$. Such a property allows multiparametric determination of the optical properties at any duration and repetition rate of the pulses, up to a continuous laser radiation. Using such a model allows makes it possible to reveal substances with threshold effect. In the case of *Z*-scanning there is a strong dependence of the intensity of the beam radius, which allows determining the beam waist radius w_0 [2].

Materials with high nonlinear absorption can be used to create passive limiters of laser radiation [7,8]. Such devices are capable of increasing the safety and reliability of laser systems. The number of laser studies increases with time, lasers are efficiently used to solve problems of medicine, industry, and science [9,10]. It is worth

separate mentioning the increasing number of lidars, which are used almost everywhere in multiple fields, such as navigation of aircrafts [11,12], autonomous vehicles [13] and mobile robots [14], bathymetry [15,16] and land topography [17,18], study of atmospheric aerosols [19], and gas detection [20]. These applications involve a wide range of wavelengths [21,22]. These devices allow increasing the maximum admissible power of laser radiation preventing damage of cameras [23,24] and light-sensitive detectors, injury of the unprotected eye retina [25,26].

1. Materials and their spectral studies

To approve the threshold model for a flattop beam, we used dispersions of single-wall carbon nanotubes (SWCNTs). The material allows laser radiation attenuation in a wide range of wavelengths, which is confirmed by studying one sample at several wavelengths [27–29]. It is possible to attach various molecules in particular, phthalocyanines [30] to SWCNTs in order to increase the nonlinear optical attenuation at the expense of combined action of a few mechanisms that contribute to the total attenuation. To achieve such results, the studied SWCNTs were decorated with nanoparticles [31,32] or functionalized with dye molecules [30,33]. It is worth noting that such nanohybrids must form sedimentation-resistant dispersions, and this problem remains urgent to date [34]. One of the ways to solve this problem is to use surface-active substances (SASs), widely used in the studies of carbon nanotubes [34–38]. In this work, we used as a SAS the sodium dodecyl sulfate (SDS) already reported earlier [35,36,39].

1.1. Materials

In the present work, we used initial SWCNTs (Uglerod ChG, Chernogolovka, Russian Federation) and the ones preliminarily purified by washing in concentrated hydrochloric acid [30]. To enhance the resistance to sedimentation, we added a SDS and mixed the dispersion with a magnetic stirrer and ultrasound. The amount of SWCNTs was chosen such that at two wavelengths $\lambda = 355$ and 532 nm the transmission of the material with the optical thickness of the layer of 3 mm would be not less than 70% and the laser radiation intensity would not exceed the threshold intensity I_{thr}. In the case of Z-scanning with open aperture, the sample position was chosen such that within 20−40 cm from the lens focal point the normalized transmission T would stay close to one. For a fixed sample, the initial conditions were specified by the input energy of the pulse, which for 355 nm and 532 nm amounted to 5 μJ and 16 μJ, respectively. A distinctive feature of the optical scheme used here compared to those of previously reported experiments [2,3,30,40] is the use of a special optical component, the laser beam shaper, which allows making it flattop at the lens focus for the above wavelengths. It is worth a special note that in the ultraviolet range such studies are much rarer and, as a rule, require special optics.

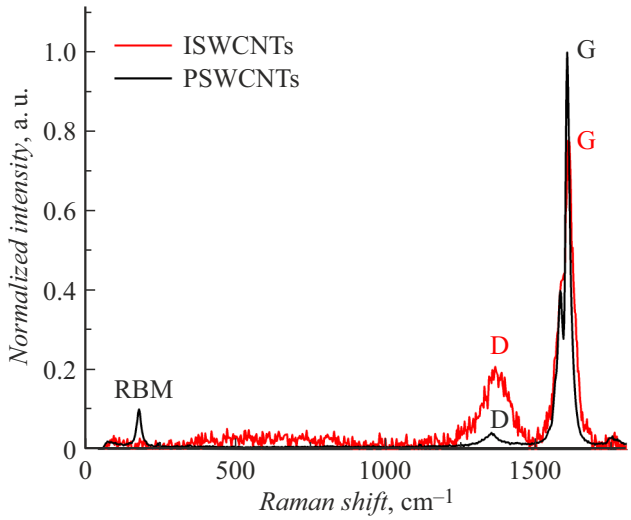

Figure 1. Raman spectrum of the initial SWCNTs (ISWCNTs) and purified ones (PSWCNTs).

1.2. Spectral studies of the used materials

Raman scattering of light has been used to diagnose SWCNTs. A small amount of nanotubes in an aqueous dispersion was preliminarily dried on a substrate. The study was carried out using laser radiation with a wavelength of 532 nm in the operating range of the Raman shift recording of 100−1800 cm^{-1} (Fig. 1). The ratio of band intensities was $I_D/I_G = 0.26$ for initial SWCNTs and decreased to $I_D/I_G = 0.04$ in the case of purified SWCNTs. These data confirm the effect of the purification procedure on SWCNTs; in addition, a band of the RBM mode was found, which is noise-hidden in the case of the original SWCNTs.

The prepared aqueous dispersions were studied by means of optical spectroscopy in the range from 250−850 nm (Fig. 2). The spectrum shows the wavelengths at which experiments were carried out to determine the nonlinear optical characteristics when testing the model. In the visible wavelength range, the absorption of dispersions with SWCNTs is maintained at almost the same level, which makes them similar to neutral light filters and indicates the possibility of using them in a wide wavelength range. When observed for a long time, up to three months, no precipitation was detected.

2. Theoretical analysis of the threshold model for a flattop beam

Despite the wide variety of models describing the relationship between the nonlinear absorption coefficient and the intensity, they are based on significant approximations; in particular, they are restricted to the mechanisms of reverse

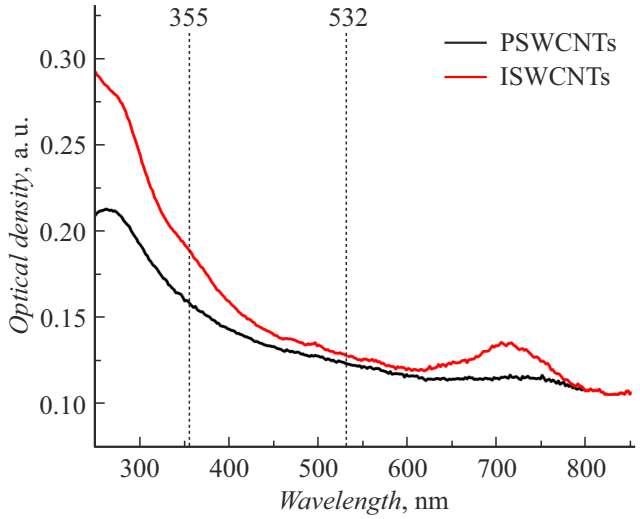

Figure 2. Optical spectra of the initial SWCNTs (ISWCNTs) and purified SWCNTs (PSWCNTs).

saturation of absorption induced by two- or three-photon absorption, as well as absorption by free carriers [41]. In this case, when induced scattering occurs, the interpretation of the results is difficult due to an increase in the optical path inside the sample giving rise to an increase in absorption [40]. For dispersions, it is possible to describe the theoretical curve more accurately using a threshold model, which also makes it possible to determine the value of the threshold intensity [3]. A new, simple analytical solution using a threshold model is obtained for the case of a beam with a flat top. Such a beam was obtained using additional optical elements as part of the laser beam shaper.

The aim of this study is to elucidate the possibilities of multiparametric determination of the optical properties of materials by two methods, one using a fixed position of the material and the other using Z-scanning with an open aperture, to calculate the effective coefficient of nonlinear absorption β_{thr}, threshold intensity I_{thr}, and the beam waist radius w_0.

2.1. Fixed material position method

The theoretical value of the transmitted intensity is determined in accordance with the radiative transfer equation (RTE) [2,3] for the nonlinear threshold dependence of the absorption coefficient on the incident intensity I_0. The intensity dependence of the absorption coefficient itself is given by effective values, since in dispersions microplasma or microbubbles can arise, which are light-scattering centers [42] and contribute to an increase in the optical path with increasing absorption [40]. With this in mind, the effective absorption coefficient $\mu(I_0)$ is defined as:

$$\mu(I_0) = \alpha_0 + \beta_{\text{eff}}(I_0 - I_{\text{thr}})\eta(I_0 - I_{\text{thr}}), \qquad (1)$$

where α_0 is the linear absorption coefficient; β_{eff} is the effective nonlinear coefficient of two-photon absorption; η is the Heaviside function, necessary to describe the threshold behavior.

The incident intensity I_0 is generally characterized by the pulse radial profile in the cross section $A(\rho)$ depending on the distance from the beam axis ρ [40]. Experimentally, the total pulse energy U_0 is determined, therefore, it is convenient to normalize the pulse profile to $1/(2\pi)$. Then for a flattop beam with constant intensity in the transverse section, we get the following expression:

$$A(\rho) = \frac{1}{w_\pi^2 \pi}\,\eta(w_\pi - \rho), \qquad (2)$$

where w_π is the radius of the flattop π-shaped beam.

The analysis of results is based on the dependence of normalized transmission T on the total energy of input pulses. To use the least-squares method (LSM), it is convenient to exploit a logarithm of normalized transmission Lt. According to Eq. (1), for a flattop beam profile (2) in the case of experiment with fixed absorber position, the theoretical values of this quantity are determined from the formula

$$Lt_N = \ln(T_N) = \beta_{\text{eff}}\frac{U_{\text{thr}} - U_{0N}}{\pi\tau w_\pi^2}\,d, \qquad (3)$$

where τ is the pulse duration, U_{thr} is the threshold total energy of the pulse, d is the material layer thickness, and N is the number of the measurement.

The direct problem is to determine the dependence of normalized transmission on the total input pulse energy using Eq. (3) for given values of the material optical properties. The inverse problem is to determine the optical parameters from the experimental dependence of the normalized transmission on the input pulse total energy. The parameters were calculated using the LSM by minimizing the sum of squared residuals. For this purpose, a function of two variables, which depends on the desired parameters is introduced:

$$S(\beta_{\text{eff}}, U_{\text{thr}}) = \sum_{i=1}^{N}\left[Lt_i + \beta_{\text{eff}}\frac{U_{0i} - U_{\text{thr}}}{\pi\tau w_\pi^2}\,d\right]^2, \qquad (4)$$

where i is the experiment number, N is the number of experimental values, Lt_i are the values of the normalized transmission logarithm determined experimentally.

A statistical study of errors was carried out using Eq. (4) in 20 parallel computational experiments using Student's t-test. Table 1 shows the data for aqueous dispersions of purified SWCNTs. In Table 1 the average values are $\beta_{\text{eff}}^{\text{av}}$ and $U_{\text{thr}}^{\text{av}}$; β_{eff}^{-}, β_{eff}^{+}, U_{thr}^{-} and U_{thr}^{+} denote the lower and upper limits of the confidence interval for these values with a significance level of 0.01.

2.2. Open aperture Z-scan method

Similarly, using the least squares method, one can determine the optical parameters and beam waist radius from the data of Z-scanning with open aperture. In this case, when the sample is displaced by z relative to the lens

Table 1. Statistical results of data analysis by the method of fixed material location

Sample	λ, nm	d, cm	β_{eff}^{-}, cm · GW^{-1}	$\beta_{\text{eff}}^{\text{av}}$, cm · GW^{-1}	β_{eff}^{+}, cm · GW^{-1}	U_{thr}^{-}, μJ	$U_{\text{thr}}^{\text{av}}$, μJ	U_{thr}^{+}, μJ
SWCNTs/water	532	0.3	98.3	101.1	103.9	15.8	16.2	16.6
SWCNTs/water	355	0.3	190.8	196.2	201.6	4.8	4.9	5.0

Table 2. Statistical results of data analysis by the Z-scan method

Sample	λ, nm	β_{eff}^{-}, cm · GW^{-1}	$\beta_{\text{eff}}^{\text{av}}$, cm · GW^{-1}	β_{eff}^{+}, cm · GW^{-1}	U_{thr}^{-}, μJ	$U_{\text{thr}}^{\text{av}}$, μJ	U_{thr}^{+}, μJ	w_0^{-}, μm	w_0^{av}, μm	w_0^{+}, μm
SWCNTs/water	532	95.6	99.6	103.6	15.8	16.2	16.6	85.4	86.7	88.0
SWCNTs/water	355	185.8	193.6	201.3	4.8	4.9	5.0	71.7	72.8	73.9

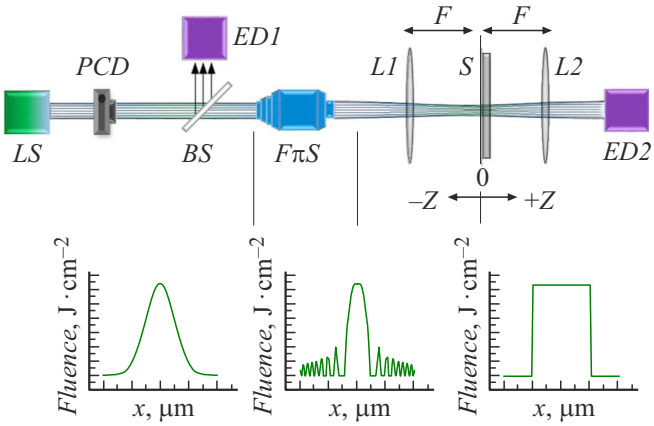

Figure 3. Optical scheme for measurements by the method of fixed sample location. Explanations are given in the text.

focus, the beam radius will change. Such a change leads to a variation in the energy flux density, and to describe this effect, the normalized beam radius is used:

$$w_n = \sqrt{1 + \frac{z^2}{z_0^2}}, \tag{5}$$

where z_0 is the Rayleigh length; for the method of fixed material position $w_n = 1$.

For open aperture Z-scan, considering Eq. (5), we get the dependence of the normalized transmission logarithm in the following form:

$$Lt_N = \beta_{\text{eff}} \frac{2}{\pi^{3/2}\tau w_0^2}\left(U_{\text{thr}} - U_0 \frac{1}{w_n^2}\right)d, \tag{6}$$

where w_0 is the beam waist radius.

Based on Eq. (6), we introduce a function of three variables for the case of Z-scanning with open aperture:

$$S(\beta_{\text{eff}}, U_{\text{thr}}, w_0) = \sum_{i=1}^{N}\left[Lt_i + \beta_{\text{eff}} \frac{2}{\pi^{3/2}\tau w_0^2}\left(U_{\text{thr}} - U_0 \frac{1}{w_n^2}\right)d\right]^2. \tag{7}$$

The results of a statistical study using Eq. (7) and Student's t-test are shown in Table 2 for aqueous dispersions of purified SWCNTs. In the case of Z-scanning with open aperture, experimental data can be used to determine the average radius of the beam in the waist w_0^{av} and the corresponding upper w_0^{+} and lower w_0^{-} boundaries of the confidence interval with the significance level 0.01.

3. Approbation of the threshold model for a flattop beam

Investigations by the method of fixed sample position were carried out using the setup schematically shown in Fig. 3. In the studies using pulsed radiation of the Gaussian shape, only focusing of the laser radiation is required for the correct tuning of the device. To obtain a single flattop pulse from a Gaussian beam, the use of a beam shaper $F\pi S$ is necessary. In the optical scheme in Fig. 3, such profile is achieved at the focus position of lenses $L1$ and $L2$ (F being the focal length), where the sample S is fixed.

According to the fixed position technique (Fig. 3), a Nd:YAG laser (Lotis Tii) at the wavelength of the second and third harmonics was used as a laser source (LS) of radiation. The laser single pulse energy was varied by a polarization-type power control device (PCD), and the input and output energies were measured by the energy detectors $ED1$ and $ED2$, respectively. To measure the input energy, part of the radiation was diverted using the beam splitter BS.

3.1. Normalized transmittance measurements using the fixed material position method

The dependences of the normalized transmission on the incident pulse total energy were determined for the dispersions of the initial SWCNTs (Fig. 4, a) and purified SWCNTs (Fig. 4, b) in water using SDS. The measurements were carried out in a quartz cell with a thickness of 3 mm. The radius of the beam incident on the sample was measured using a CCD camera with the position of the

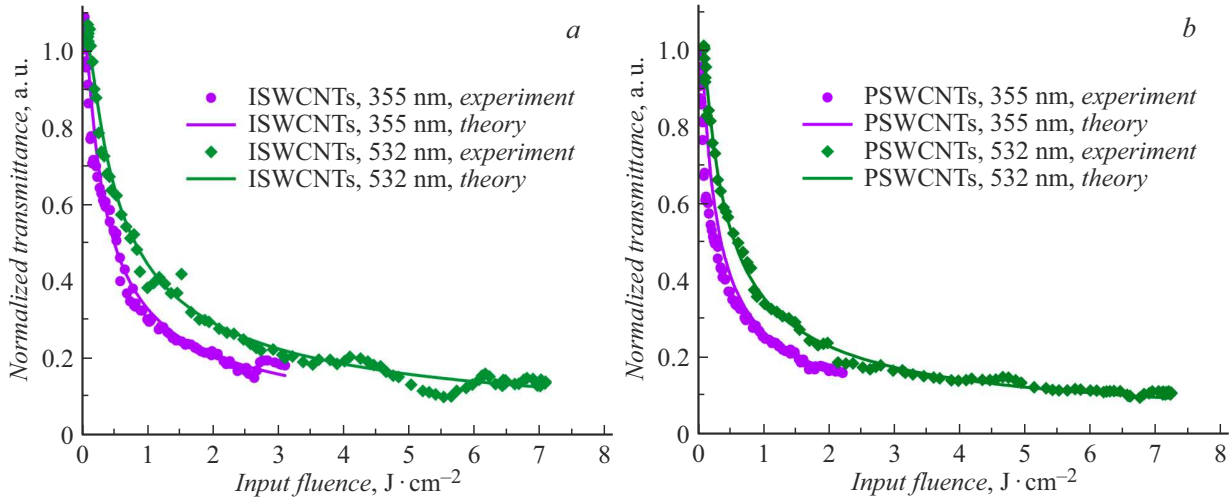

Figure 4. Dependence of the normalized transmission on the incident total pulse energy at wavelengths of 532 and 355 nm for initial ISWCNTs (*a*) and purified PSWCNTs (*b*).

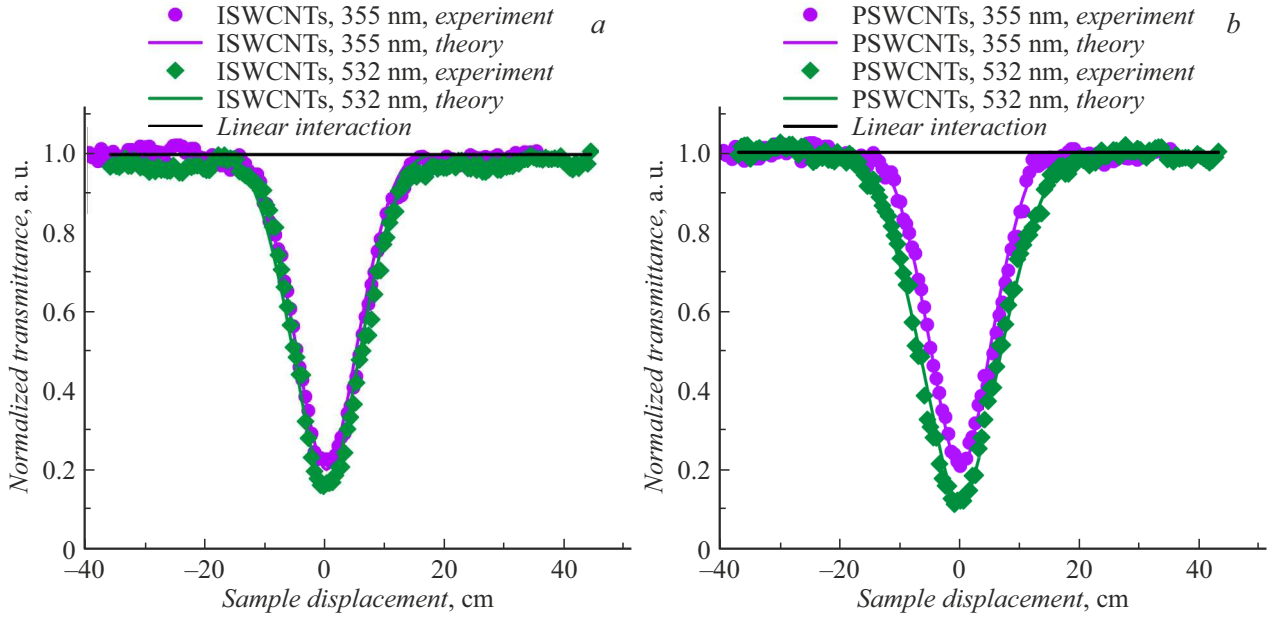

Figure 5. Dependence of the normalized transmission on the displacement of the sample relative to the lens focus at wavelengths of 532 and 355 nm for the initial ISWCNTs (*a*) SWCNTs and the purified PSWCNTs (*b*) SWCNTs.

sensitive matrix taken into account. The measurements were carried out in the range of the input single pulse total energy $0.5-300\,\mu$J at a wavelength of 532 nm and $0.5-100\,\mu$J at a wavelength of 355 nm, respectively, for all samples . The maximum energy corresponded to the destruction threshold of the quartz cell.

3.2. Measurements of the normalized transmission using the *Z*-scan method with an open aperture

When performing measurements using the *Z*-scan method with an open aperture, the scheme described earlier [3,31] was used. The dispersions of the original SWCNTs (Fig. 5, *a*) and purified SWCNTs (Fig. 5, *b*) in water using SDS were studied. The measurements were performed at a fixed input single pulse total energy of 300 and $100\,\mu$J at wavelengths of 532 and 355 nm, respectively, with a sample displacement step of 0.5 mm for all samples.

3.3. Results

The discrepancy between the parameters was determined by the two described methods, which shows the possibility of using these measurement techniques using a new threshold model for the case of a beam with a flat top

Table 3. Comparison of the parameter values of different dispersions at two wavelengths by two methods

Sample(λ)	Parameters	Value of parameters for method of fixed location of sample and CCD camera	Value of parameters for method of *Z*-scan	Discrepancy of values of parameters
Initial SWCNTs/water (532 nm)	β_{eff}, cm · GW^{-1}	78.3	78.1	0.2
	U_{thr}, μJ	16.3	16.5	0.2
	w_0, μm	82.0	81.6	0.4
	DR, a.u.	18.4	18.2	0.2
	CA, a.u.	8.3	8.1	0.2
Initial SWCNTs/water (355 nm)	β_{eff}, cm · GW^{-1}	152.1	151.7	0.4
	U_{thr}, μJ	5.1	5.0	0.1
	w_0, μm	69.1	68.5	0.6
	DR, a.u.	19.6	20.0	0.4
	CA, a.u.	5.7	5.4	0.3
Purified SWCNTs/water (532 nm)	β_{eff}, cm · GW^{-1}	99.2	98.9	0.3
	U_{thr}, μJ	16.2	16.5	0.3
	w_0, μm	86.0	85.7	0.3
	DR, a.u.	18.5	18.2	0.3
	CA, a.u.	11.1	10.9	0.2
Purified SWCNTs/water (355 nm)	β_{eff}, cm · GW^{-1}	196.0	192.9	3.1
	U_{thr}, μJ	4.9	5.0	0.1
	w_0, μm	72.6	72.4	0.2
	DR, a.u.	20.4	20.0	0.4
	CA, a.u.	6.6	6.4	0.2

(Table 3). The linear absorption coefficient for all samples was 1.46 cm^{-1} at a wavelength of 532 nm and 1.87 cm^{-1} at 355 nm. Also presented in Table 3 are the values of the dynamic range *DR*, which is a ratio of maximum and threshold total energy values of a single pulse, and the attenuation coefficient *CA*, which characterizes the maximal attenuation as compared to the initial transmission.

Conclusion

The threshold model for the case of a beam with a flat top makes it possible to determine the optical parameters and the radius of the beam using the fixed sample location methods and the *Z*-scan method with an open aperture. The beam shaper scheme ensures a flattop beam profile. Determination of optical parameters using a threshold model in the case of a flattop beam allows measurements of SWCNT dispersions and can be used to study samples with unknown optical properties. For a flattop beam, a new exact analytical solution in elementary functions is derived, which cannot be obtained for the general case of a Gaussian beam. The new approach makes it possible to describe the nonlinear interaction of laser radiation with a material at a uniform intensity distribution over the cross section, which was achieved by means of a beam shaper. At the same time, the exact solution in elementary functions reduces the number of arithmetic and logical operations in numerical methods and reduces the requirements for computing speed. The possibility of constructing a theoretical curve for the case of *Z*-scanning with an open aperture is shown by introducing the normalized transmission, which characterizes the change in the beam radius behind the lens for a variable position of the sample relative to the focus.

Measurements at wavelengths of 355 and 532 nm show the possibility of using SWCNT dispersions to attenuate laser radiation due to nonlinear effects. The use of purified SWCNTs allows achieving high values of the effective nonlinear absorption coefficient, while the use of SDS

reduces the SWCNT aggregation (twisting into bundles). Dispersions of purified SWCNTs are better suited for creating nonlinear optical elements for passive limiters of laser radiation with a confocal sample arrangement. Such materials attenuate laser radiation from a source with a pulse duration of 20 ns and a response time less than the duration of the pulses themselves. The corresponding rate exceeds the speed of any active device for protection against high power laser radiation.

Funding

The preparation of samples resistant to sedimentation and analytical calculations were supported by the Russian Science Foundation (grant 21-73-20016). Research on the protection of photosensitive detectors and CCD arrays using single-walled carbon nanotubes was supported by the Ministry of Industry and Trade of the Russian Federation (State Contract № 20411.1950192501.11.003 dated December 29, 2020, ID 17705596339200009540).

Conflict of interest

The authors declare that they have no conflict of interest.

References

[1] M. Sheik-Bahae, A.A. Said, T.-H. Wei, D.J. Hagan, E.W. Van Stryland. IEEE J. Quantum Electron, **26** (4), 760 (1990). DOI: 10.1109/3.53394
[2] S.A. Tereshchenko, V.M. Podgaetskii, A.Y. Gerasimenko, M.S. Savel'ev. Opt. Spectr., **116** (3), 454 (2014). DOI: 10.1134/S0030400X14030217
[3] S.A. Tereshchenko, M.S. Savelyev, V.M. Podgaetsky, A.Y. Gerasimenko, S.V. Selishchev. J. Appl. Phys., **120** (9), 093109 (2016). DOI: 10.1063/1.4962199
[4] A.A. Said, M. Sheik-Bahae, D.J. Hagan, T.H. Wei, J. Wang, J. Young, E.W. Van Stryland. J. Opt. Soc. Am. B, **9** (3), 405 (1992). DOI: 10.1364/JOSAB.9.000405
[5] G. Račiukatis. J. Laser Micro/Nanoengineering, **6** (1), 37 (2011). DOI: 10.2961/jlmn.2011.01.0009
[6] X.G. Huang. Opt. Eng., **38** (2), 208 (1999). DOI: 10.1117/1.602255
[7] G. Zhang, I.W. Primaatmaja, J.Y. Haw, X. Gong, C. Wang, C.C.W. Lim. *Quantum Information and Measurement VI 2021* (Washington, D.C., Optica Publishing Group, 2021), p. M2C.6. DOI: 10.1364/QIM.2021.M2C.6
[8] H. Qian, S. Li, Y. Li, C.-F. Chen, W. Chen, S.E. Bopp, Y.-U. Lee, W. Xiong, Z. Liu. Sci. Adv., **6** (20), (2020). DOI: 10.1126/sciadv.aay3456
[9] M. Veisi, S. H. Kazemi, M. Mahmoudi. Sci. Rep., **10** (1), 16304 (2020). DOI: 10.1038/s41598-020-73343-2
[10] H. Fan, X. Wang, Q. Ren, X. Zhao, G. Zhang, J. Chen, D. Xu, G. Yu, Z. Sun. Opt. Laser Technol., **42** (5), 732 (2010). DOI: 10.1016/j.optlastec.2009.11.017.
[11] L. Zheng, P. Zhang, J. Tan, F. Li. IEEE Access, **7**, 163437 (2019). DOI: 10.1109/ACCESS.2019.2952173
[12] R. Zhou, W. Jiang, S. Jiang. Remote Sens., **10** (12), 2051 (2018). DOI: 10.3390/rs10122051
[13] S. Royo, M. Ballesta-Garcia. Appl. Sci., **9** (19), 4093 (2019). DOI: 10.3390/app9194093
[14] M. Hasan, J. Hanawa, R. Goto, H. Fukuda, Y. Kuno, Y. Kobayashi. IEEJ Trans. Electr. Electron. Eng., **16** (5), 778 (2021). DOI: 10.1002/tee.23358
[15] L. Janowski, R. Wroblewski, M. Rucinska, A. Kubowicz-Grajewska, P. Tysiac. Eng. Geol., **301**, 106615 (2022). DOI: 10.1016/j.enggeo.2022.106615
[16] G. Mandlburger, M. Pfennigbauer, R. Schwarz, S. Flöry, L. Nussbaumer. Remote Sens., **12** (6), 986 (2020). DOI: 10.3390/rs12060986
[17] S.M. Marselis, K. Abernethy, A. Alonso, J. Armston, T.R. Baker, J. Bastin, J. Bogaert, D.S. Boyd, P. Boeckx, D.F.R.P. Burslem, R. Chazdon, D.B. Clark, D. Coomes, L. Duncanson, S. Hancock, R. Hill, C. Hopkinson, E. Kearsley, J.R. Kellner, D. Kenfack, N. Labriére, S.L. Lewis, D. Minor, H. Memiaghe, A. Monteagudo, R. Nilus, M. O'Brien, O.L. Phillips, J. Poulsen, H. Tang, H. Verbeeck, R. Dubayah. Glob. Ecol. Biogeogr., **29** (10), 1799 (2020). DOI: 10.1111/geb.13158
[18] A.E. Thompson. Remote Sens., **12** (17), 2838 (2020). DOI: 10.3390/rs12172838
[19] J. Shen, N. Cao, Y. Zhao. Optik (Stuttg). **227**, 165980 (2021). DOI: 10.1016/j.ijleo.2020.165980
[20] T. Shiina. *Ionizing Radiation Effects and Applications,* ed. by B. Djezzar (IntechOpen, London, United Kingdom, 2018), p. 186. DOI: 10.5772/intechopen.74630
[21] C. Jiang, Y. Chen, W. Tian, Z. Feng, W. Li, C. Zhou, H. Shao, E. Puttonen, J. Hyyppä. Satell. Navig., **1** (1), 29 (2020). DOI: 10.1186/s43020-020-00029-5
[22] E. Garmire. Opt. Express, **21** (25), 30532 (2013). DOI: 10.1364/OE.21.030532
[23] W.M. Elwekeel, A. Salah, T. Ismail, H. Selmy, M. Alshershby, Y.A. Badr, B. Anis. Opt. Mater. (Amst), **122**, 111732 (2021). DOI: 10.1016/j.optmat.2021.111732
[24] B. Schwarz, G. Ritt, M. Koerber, B. Eberle. Opt. Eng., **56** (3), 034108 (2017). DOI: 10.1117/1.OE.56.3.034108
[25] M. Zhang, X. Xu, J. Liu, Y. Jiang, J. Wang, N. Dong, C. Chen, B. Zhu, Y. Liang, T. Fan, J. Xu. ACS Appl. Mater. Interfaces, **14** (29), 33787 (2022). DOI: 10.1021/acsami.2c06476
[26] T.C. Sabari Girisun, M. Saravanan, S. Venugopal Rao. J. Appl. Phys., **124** (19), 193101 (2018). DOI: 10.1063/1.5050478
[27] Y. Chen, Y. Lin, Y. Liu, J. Doyle, N. He, X. Zhuang, J. Bai, W.J. Blau. J. Nanosci. Nanotechnol., **7** (4), 1268 (2007). DOI: 10.1166/jnn.2007.308
[28] K.C. Chin, A. Gohel, H.I. Elim, W. Chen, W. Ji, G.L. Chong, C.H. Sow, A.T.S. Wee. J. Mater. Res., **21** (11), 2758 (2006). DOI: 10.1557/jmr.2006.0338
[29] L. Vivien, D. Riehl, P. Lançon, F. Hache, E. Anglaret. Opt. Lett., **26** (4), 223 (2001). DOI: 10.1364/OL.26.000223
[30] M.S. Savelyev, A.Y. Gerasimenko, V.M. Podgaetskii, S.A. Tereshchenko, S.V. Selishchev, A.Y. Tolbin. Opt. Laser Technol., **117**, 272 (2019). DOI: 10.1016/j.optlastec.2019.04.036
[31] F.H. Alkallas, H.A. Ahmed, R. Adel Pashameah, S.H. Alrefaee, A. Toghan, A. Ben Gouider Trabelsi, A.M. Mostafa. Opt. Laser Technol., **155**, 108444 (2022). DOI: 10.1016/j.optlastec.2022.108444
[32] T.A. Alrebdi, H.A. Ahmed, F.H. Alkallas, E.A. Mwafy, A.B.G. Trabelsi, A.M. Mostafa. Radiat. Phys. Chem., **195**, 110088 (2022). DOI: 10.1016/j.radphyschem.2022.110088

[33] A. Wang, L. Cheng, W. Zhao, W. Zhu, D. Shang. Dye. Pigment., **161**, 155 (2019). DOI: 10.1016/j.dyepig.2018.09.057
[34] B.I. Kharisov, O.V. Kharissova, H. Leija Gutierrez, U. Ortiz Méndez. Ind. Eng. Chem. Res., **48** (2), 572 (2009). DOI: 10.1021/ie800694f
[35] D. Bouchard, X. Chang, I. Chowdhury. Environ. Nanotechnology, Monit. Manag., **4**, 42 (2015). DOI: 10.1016/j.enmm.2015.07.001
[36] M. Davoodabadi, M. Liebscher, S. Hampel, M. Sgarzi, A.B. Rezaie, D. Wolf, G. Cuniberti, V. Mechtcherine, J. Yang, Compos. Part B Eng., **209**, 108559 (2021). DOI: 10.1016/j.compositesb.2020.108559
[37] R. Rastogi, R. Kaushal, S.K. Tripathi, A.L. Sharma, I. Kaur, L.M. Bharadwaj. J. Colloid Interface Sci., **328** (2), 421 (2008). DOI: 10.1016/j.jcis.2008.09.015
[38] Yu.N. Tolchkov, T.I. Panina, Z.A. Mikhaleva, E.V. Galunin, N.R. Memetov, A.G. Tkachev. Khimicheskaya fizika i mezoskopiya, **19** (2), 292 (2017) (in Russian).
[39] O.S. Zueva, O.N. Makshakova, B.Z. Idiyatullin, D.A. Faizullin, N.N. Benevolenskaya, A.O. Borovskaya, E.A. Sharipova, Yu.N. Osin, V.V. Salnikov, Yu.F. Zuev. Izvestiya AN, seriya khimicheskaya **5**, 1208 (2016) (in Russian).
[40] M.S. Savelyev, A.Y. Gerasimenko, P.N. Vasilevsky, Y.O. Fedorova, T. Groth, G.N. Ten, D.V. Telyshev. Anal. Biochem., **598**, 113710 (2020). DOI: 10.1016/j.ab.2020.113710
[41] L.W. Tutt, T.F. Boggess. Prog. Quantum Electron., **17** (4), 299 (1993). DOI: 10.1016/0079-6727(93)90004-S
[42] Q. Zhang, Y. Qiu, F. Lin, C. Niu, X. Zhou, Z. Liu, M.K. Alam, S. Dai, W. Zhang, J. Hu, Z. Wang, J. Bao. Nanoscale, **12** (13), 7109 (2020). DOI: 10.1039/C9NR10516F

Translated by Ego Translating